

Microscopic properties of fractional vortices and domain walls in three-band $s + is$ superconductors

Igor Timoshuk and Egor Babaev

*Department of Physics, The Royal Institute of Technology, Stockholm SE-10691, Sweden and
Wallenberg Initiative Materials Science for Sustainability, Department of Physics,
The Royal Institute of Technology, Stockholm SE-10691, Sweden*

We report microscopic solutions for vortices carrying a variable fraction of magnetic flux quantum and domain walls in a three-band $s + is$ superconductor and investigate their properties. The solutions are obtained in a fully self-consistent treatment of the three-band Bogoliubov-de-Gennes model.

I. INTRODUCTION

The flux quantization is a fundamental property of conventional superconductors [1, 2]. In London’s argument, the flux quantization is a consequence of the quantization of the circulation of the 2π -periodic phase variable, called the phase winding $\oint \nabla\theta = 2\pi N$ where N is an integer. At a deeper level, the existence of the phase comes as a consequence of the concept that a superconductor is a state of matter that spontaneously breaks $U(1)$ gauge symmetry and, hence, is described by a complex order parameter field [3, 4]. These circumstances ensure that in an infinite sample, there are no stable solutions violating the quantization [5]. Similar symmetry-based arguments were used to predict that chiral p -wave superconductors allow half-quantum vortices [6, 7]. A different proposal was made in [8], where it was suggested that in contrast to symmetry-based arguments, vorticity could exist in a gap field of an individual band of a multiband superconductor. In that case, a vortex can carry an arbitrary fraction of magnetic flux quantum (recently, such vortices were termed unquantized vortices). A gap field in an individual band is not an order parameter in Landau’s theory sense. Namely, adhering to symmetry-based Landau theory would imply only one order parameter since only one symmetry is broken. Hence, it would imply the presence of only one phase field, precluding the existence of vortices that carry an arbitrary fraction of magnetic flux quantum. Namely, in the conventional argument, a classical field — the order parameter — should describe all macroscopic aspects of motion regardless of microscopic detail; the number of bands is one of such ostensibly inconsequential microscopic detail.

On the other hand, a classical field theory concept is more general than an order parameter concept and does not necessarily require a set of broken symmetries. The initial constructions of “unquantized” vortex in [8] in a two-band model with single broken symmetry relied on several assumptions. Firstly, in the presence of the Josephson coupling between components of a two-component model, there are no well-defined multiple “Mexican hat” effective potentials with multiple degenerate valleys. Hence, one cannot define two phase variables using the usual symmetry principles. Nonetheless, it was argued, at the level of phenomenological models in [8],

that there can be a “deformed” and “non-degenerate” valley in the landscape of a free energy functional that still allow the introduction of two classical phase-like variables and sustain energetically stable windings in the phase variables. The recent experiment [9] reported the observation of vortices carrying a temperature-dependent fraction of the flux quantum in $\text{Ba}_{1-x}\text{K}_x\text{Fe}_2\text{As}_2$. Notably, the experiments demonstrated that the objects with fractional flux (i) can be created in various locations of the samples, giving consistent flux fractions irrespective of their position, (ii) vortices are mobile, and their position can be manipulated (iii) it was possible to create fractional and integer vortices at the same position, which proves that the observations are not artifacts of some crystal defects. More recently, vortex core fractionalization was observed in a related material KFe_2As_2 [10]. Besides the fact that the phenomenon is interesting on its own, the vortices should exhibit anyonic statistics. That is, according to the earlier work [11], a composite object of arbitrary flux tube and electron is an anyon [11–14]. Hence, due to vortex core states, the unquantized vortices physically realize such an object in a superconductor and, hence, should obey fractional statistics.

The material $\text{Ba}_{1-x}\text{K}_x\text{Fe}_2\text{As}_2$ where fractional vortices were observed is a multiband, spin-singlet superconductor. At the doping value $x \approx 0.77$, it breaks the time-reversal symmetry [15, 16]. The time-reversal symmetry is broken above the superconducting phase transition [17, 18], due to fluctuation effects [19–21]. This means that there are at least two components in the order parameters when the system transitions to the diamagnetic state. However, the situation is more complex even in the case of multiple broken symmetries in multiband superconductors. By the same argument as discussed above, more than two phase-like variables are possible in $\text{Ba}_{1-x}\text{K}_x\text{Fe}_2\text{As}_2$, despite only two broken symmetries, which implies possibly more than two kinds of fractional vortices [8, 22, 23]. It is still a subject of current experimental research how many types of fractional vortices can exist in $\text{Ba}_{1-x}\text{K}_x\text{Fe}_2\text{As}_2$.

Since the existence of “unquantized vortices” cannot be guaranteed by symmetry, and instead, one relies on interaction to produce a particular energy landscape, a detailed microscopic investigation of an isolated vortex solution is warranted. We present such solutions in a

fully self-consistent microscopic model, including inter-component gauge-field coupling. A similar solution was obtained in the Bogoliubov- de Gennes (BdG) model in [9], but only a few characteristics were studied. This work reports a detailed numerical investigation of the unquantized vortices and their properties.

II. MODEL

We focus on a three-band model where the interband Josephson coupling ensures that the model has only a single local $U(1)$ symmetry spontaneously broken. We define this model on a two-dimensional square lattice, described by the microscopic Hamiltonian

$$H = - \sum_{\alpha\sigma} \sum_{\langle ij \rangle} \exp\{iqA_{ij}\} c_{i\sigma\alpha}^\dagger c_{j\sigma\alpha} - \sum_{i\alpha\beta} V_{\alpha\beta} c_{i\uparrow\alpha}^\dagger c_{i\downarrow\alpha}^\dagger c_{i\downarrow\beta} c_{i\uparrow\beta}. \quad (1)$$

Here $\langle ij \rangle$ denotes nearest neighbor pairs, and $c_{i\sigma\alpha}$ is the fermionic annihilation operator at position i , with spin σ ($\sigma \in \{\uparrow, \downarrow\}$) and in band α ($\alpha \in \{1, 2, 3\}$), phase factor $\exp\{iqA_{ij}\}$ accounts for interaction with the magnetic vector potential $A_{ij} = \int_j^i \mathbf{A} \cdot d\mathbf{l}$ through Peierls substitution [24, 25]. The quartic interaction term, defined by $V_{\alpha\beta} = V_{\beta\alpha}^*$, allows Cooper pairs to form and tunnel between bands. Inter-band coupling dictates no extra $U(1)$ degeneracies. We consider repulsive inter-band Josephson coupling so that the model also breaks time-reversal symmetry [26, 27] to make the connection with $\text{Ba}_{1-x}\text{K}_x\text{Fe}_2\text{As}_2$ [15, 16]. The model has two broken symmetries but three components. Hence, three types of fractional vortices in this model cannot be justified by the standard “ground state manifold”-based topological classification of defects.

By performing the mean field approximation in the Cooper channel, we obtain the mean-field Hamiltonian

$$\mathcal{H} = - \sum_{\sigma\alpha} \sum_{\langle ij \rangle} \exp\{iqA_{ij}\} c_{i\sigma\alpha}^\dagger c_{j\sigma\alpha} + \sum_{i\alpha} \left(\Delta_{i\alpha} c_{i\uparrow\alpha}^\dagger c_{i\downarrow\alpha}^\dagger + \text{H.c.} \right) + \frac{1}{2} \sum_{\text{plaquettes}} B_z^2, \quad (2)$$

$$\Delta_{i\alpha} = \sum_{\beta} V_{\alpha\beta} \langle c_{i\uparrow\beta} c_{i\downarrow\beta} \rangle, \quad (3)$$

where H.c. denotes Hermitian conjugation. Discrete version of Maxwell’s equation $\nabla \times \nabla \times \mathbf{A} = \mathbf{J}$ determines the connection between A_{ij} and J_{ij}

$$J_{ij} = -2q \sum_{\alpha\sigma} \text{Im} \left\{ \langle c_{i\sigma\alpha}^\dagger c_{j\sigma\alpha} \rangle \exp\{iqA_{ij}\} \right\}. \quad (4)$$

The free energy for the system Eq. (2) can be calcu-

lated as

$$F_H = \sum_i \Delta_i^\dagger V^{-1} \Delta_i - k_B T \text{Tr} \ln (e^{-\beta\mathcal{H}} + 1) + \frac{1}{2} \sum_{\text{plaquettes}} B^2, \quad (5)$$

where the magnetic field $B = \nabla \times \mathbf{A}$ is defined on plaquettes.

Using the iteration scheme, described in [23], the solution for equations Eq. (3), Eq. (4), along with the Maxwell equation, are obtained. We used the approximate Chebyshev spectral expansion method. The self-consistent iteration procedure stops when the convergence criteria $|\delta p / (p + \epsilon)| < \epsilon$ is achieved for each of the parameters $\Delta_1, \Delta_2, \Delta_3$ and A simultaneously.

After obtaining a self-consistent solution for Δ_α and A , the tunneling conductance in the system may be found as

$$\frac{\partial I_{i\alpha}(V)}{\partial V} \propto \sum_n \left[|u_{in}|^2 f'(E_n - qV) + |v_{in}|^2 f'(E_n + qV) \right] \quad (6)$$

where f' is a derivative of the Fermi-function, i indicates the lattice point, n denotes eigenstate of the system and V is applied voltage [28–30].

III. RESULTS

This paper analyzes the solutions for square systems with linear sizes up to $L = 64$ nodes. We consider system with symmetric intraband interaction $V_{11} = V_{22} = V_{33} = 2.4$ and negative interband coupling $V_{12} = V_{13} = V_{23} = -0.6$ with fixed dimensionless charge $q = 0.25$ and various temperatures. We also investigate case of slightly non-symmetric intraband interaction $V_{11} = 2.5, V_{22} = V_{33} = 2.4, V_{12} = V_{13} = V_{23} = -u$ for $u = 0.6, 0.3, 0.1$. $\epsilon = 10^{-8}, \epsilon = 10^{-6}$ are selected as convergence parameters for all simulations.

We start the iteration procedure with an initial guess for the superconducting gaps Eq. (3) and vector potential A and converge to a self-consistent solution. Here, we consider four types of initial conditions, yielding different objects. To obtain a uniform solution without any vortex or domain wall, we set $\Delta_{i1} = 0.1, \Delta_{i2} = 0.1 \cdot e^{2\pi i/3},$ and $\Delta_{i3} = 0.1 \cdot e^{-2\pi i/3}$. A domain wall is generated by the same initial guess in the upper half of the sample, and with $\Delta_{i2} = 0.1 \cdot e^{-2\pi i/3}, \Delta_{i3} = 0.1 \cdot e^{2\pi i/3}$ in the lower one. For conventional single-flux-quanta vortex each gap was initialized as $\Delta_{i\alpha} = \tanh(20r_i/L) \cdot e^{i\varphi_i + 2\pi\alpha/3}$, where r_i and φ_i are spherical coordinates with $r = 0$ corresponding to the center of the sample and L is the system size. Unquantized vortex is generated by setting $\Delta_{i1} = \tanh(20r_i/L) \cdot e^{i\varphi_i}$ and two other bands the same as for the uniform case. The vector potential is set to

zero in the initial conditions in all four cases. Upon convergence, the domain wall is stable because of geometric pinning. To ensure that the vortex ansatz-initiated configuration converges to a stable vortex solution, we choose a significantly large grid size relative to solution size so that the interaction of the vortex with a boundary is smaller than the numerical grid pinning or numerical accuracy.

A. Vortex structure

There is a significant difference between the fractional vortex solutions for systems with (FIG. 2) and without (FIG. 1) Josephson coupling. Let us define “partial” currents as

$$J_{ij\alpha} = -2q \sum_{\sigma} \text{Im} \left\{ \left\langle c_{i\sigma\alpha}^{\dagger} c_{j\sigma\alpha} \right\rangle \exp\{iqA_{ij}\} \right\}. \quad (7)$$

In a system where particle transitions between bands ($V_{\alpha,\beta} = 0$ if $\alpha \neq \beta$) are forbidden, intercomponent interaction is induced only by coupling the vector potential, so the currents are associated with the independently conserved components for the $U(1)^3$ case (FIG. 1). One can see from the solutions that the component with the phase winding has a clockwise circulation of current. The other two components have counter-clockwise circulating currents because they do not have phase winding, and the current is due only to vector potential (note also the different magnitude of the current near the vortex core for components without phase winding). That coexistence of clock- and anti-clock-wise circulation is closely connected with the fractionalization of flux quantum. Another aspect that can be seen from the solutions is that the individual currents slowly decrease away from the vortex core, but the total current is strongly localized. The fact that far from the fractional vortex core, there are oppositely circulating currents in different components is the reason why the fractional vortex in this model has logarithmically divergent energy, as discussed in a different formalism based on macroscopic London model in [8].

When interband Josephson coupling leads to spontaneous breaking of time-reversal symmetry, the axial symmetry of partial currents breaks down, shown on FIG. 2. As will be clear from the images below, oppositely directed partial currents are associated with the interband phase-difference gradients induced by the domain walls emitted by a vortex.

B. Domain wall

Negative inter-component coupling makes the ground state of the system frustrated. When all three bands are identical, there are two possible ground states - with phases of the components $\phi_1 - \phi_2 = \phi_2 - \phi_3 = 2\pi/3$ and $\phi_1 - \phi_2 = \phi_2 - \phi_3 = -2\pi/3$. If both phase-locking states

coexist in the system, a domain wall is formed between the phases.

FIG. 2 shows that on the domain wall, two of the gaps are suppressed, and the third one is enhanced. So, if the bands are not symmetric, different kinds of domain walls may emerge. Such domain walls can, in general, have different energies per unit length. As an example, we calculated domain wall energy $E = E_{\text{DW}} - E_{\text{U}}$ for several Josephson couplings FIG. 3. Here E_{DW} stands for the total free energy Eq. (5) of a system with a domain wall, and E_{U} is the total free energy of an empty system. According to our results, if one of the gaps in the system has a larger amplitude, the domain wall, on which this gap is enhanced, has lower energy than a domain wall, where this gap is suppressed. Let us call the first kind on the domain wall a low energy (LE) domain wall, and the second kind - a high energy (HE) domain wall.

The fractional vortex may be viewed as a junction point between two different domain walls. If these walls have different energies per unit length, effective force, proportional to the energy difference, will be applied to the vortex. That can make vortices with winding on some bands harder to stabilize by pinning.

C. Tunneling conductance

Scanning Tunneling Microscopy is a powerful technique for studying vortices, e.g. [31, 32]. In our model, tunneling conductance may be calculated using Eq. (6). The first question is how observable domain walls in $s + is$ superconductors are via their density-of-states signatures.

FIG. 4 represents tunneling conductance curves for high energy (HE) and low energy (LE) domain walls, compared with tunneling conductance dependence in domain-wall-free samples. Domain walls for certain coupling strength u have noticeable suppression of the gaps and thus may be observed in STM. The domain wall conductance is higher than the bulk conductance below the superconducting gap and lower above the gap. It may also be seen that the patterns for both kinds of domain walls are pretty similar.

FIG. 5 demonstrates a significant difference between fractional and conventional vortex in $U(1)^3$ and $U(1) \times Z_2$ systems arising due to very different core structures.

D. Magnetic field

In general, the shape and localization of the magnetic field of a fractional vortex in these models depend on the temperature and the strength of inter-component Josephson coupling.

It was pointed out in the $U(1) \times U(1)$ Ginzburg-Landau models that general fractional vortices have power-law localization of the magnetic flux [33]. Also, clear differences in the magnetic field location of fractional ver-

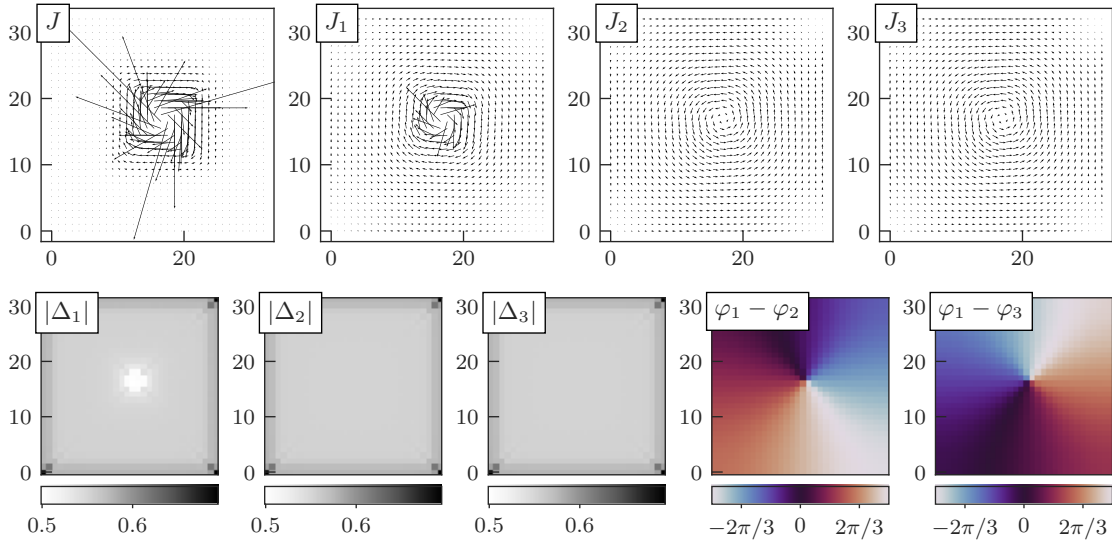


FIG. 1. Unquantized vortex with phase winding only in the first phase in a $U(1)^3$ three-component model. Current distribution Eq. (4) J , partial currents Eq. (7) J_1 , J_2 , J_3 , absolute gap values Δ_1 , Δ_2 , Δ_3 , and relative gap phases $\varphi_1 - \varphi_2$ and $\varphi_1 - \varphi_3$ are demonstrated. Square sample with linear size 32 with intraband coupling $V_{11} = V_{22} = V_{33} = 2.4$, zero interband coupling, $T = 0.12$ and $q = 0.25$ is simulated.

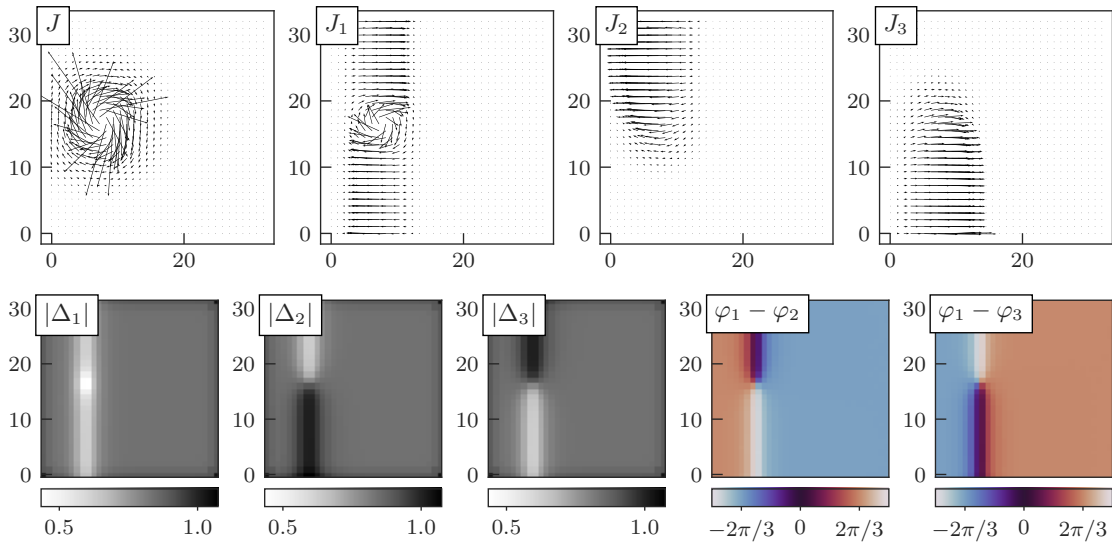


FIG. 2. Unquantized vortex in a $U(1) \times Z_2$ three-component model. Model parameters are the same, as FIG. 1, except interband coupling $V_{12} = V_{13} = V_{23} = -0.6$ and temperature $T = 0.36$. On the domain wall, away from the vortex, partial currents compensate, and the total current is zero

sus integer vortices were observed in the experiment [9]. In the case of the Josephson-coupled system, the phase-difference mode is massive. Hence, we expect an exponential localization, but the overall localization can differ.

Concerning the shape of the magnetic field, the following patterns can be observed - conventional vortex in both interacting and non-interacting systems is rotationally symmetric (apart from some corrections related to

the square symmetry of our grid) and carries one quantum of magnetic flux FIG. 6, 7. The unquantized vortex carries $1/3$ quanta in both cases due to the chosen symmetry between the components. However, in the presence of Josephson coupling, it generally tends to elongate along the domain wall.

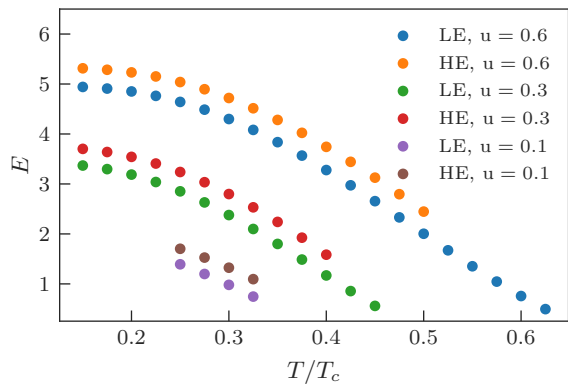


FIG. 3. Domain wall energy in bandwidth units as a function of temperature. Domain wall was generated in the middle of a square sample with 24×24 nodes. Results were obtained for slightly asymmetric intraband coupling $V_{11} = 2.5$, $V_{22} = V_{33} = 2.4$ and various interband couplings $V_{12} = V_{13} = V_{23} = -u$, $u = 0.6, 0.3, 0.1$. The energy is calculated for both kinds of domain walls - high energy (HE) and low energy (LE). A characteristic temperature exists for each coupling strength, above which the HE domain wall becomes unstable on our numerical grid. For higher temperatures, domain wall width becomes comparable with the system size.

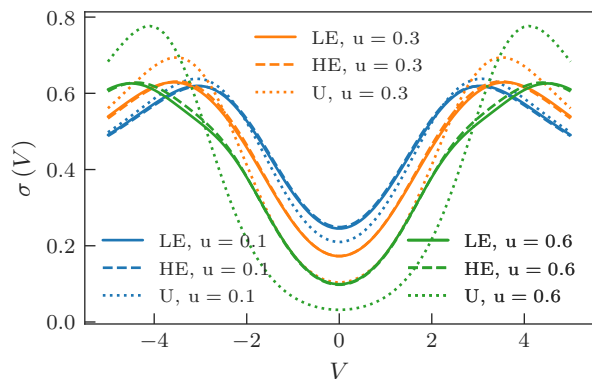


FIG. 4. Tunneling conductance Eq. (6) for different domain walls and uniform solution (U). Simulation parameters are the same as on FIG. 3, $T = 0.25T_c$. For weak interband coupling $s + is$, the domain wall gives nearly no signature in tunneling conductance.

IV. DISCUSSION

The observation of vortices that carry a varying fraction of quantum flux (unquantized vortices) in the multi-band superconductor $\text{Ba}_{1-x}\text{K}_x\text{Fe}_2\text{As}_2$ requires a theoretical understanding of these objects. The non-trivial aspect of this material is the existence of only two broken symmetries but at least three superconducting bands. According to the Ginzburg-Landau and London models-based arguments [8, 22], this circumstance may lead to more than two fractional vortices. One cannot justify

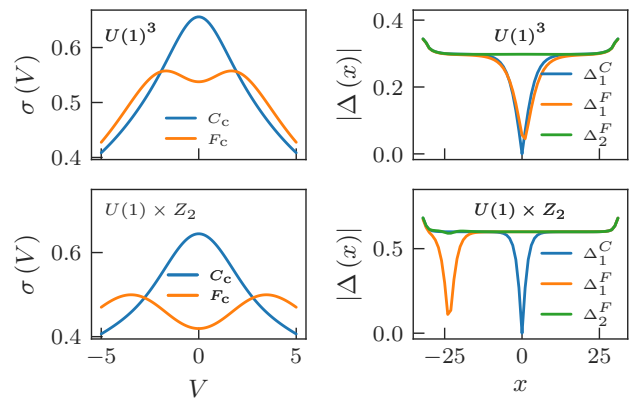


FIG. 5. Tunneling conductance $\sigma(V)$ Eq. (6) for conventional (C_c) and fractional (F_c) vortex cores and gap amplitude crosssections in $U(1)^3$ and $U(1) \times Z_2$ systems. A square sample with a linear size of 64 nodes was analyzed for a system with couplings $V_{11} = V_{22} = V_{33} = 2.4$ and charge $q = 0.25$. For $U(1)^3$ system temperature $T = 0.37$ and zero intercomponent coupling was used; for $U(1) \times Z_2$ system $T = 0.27$ and intercomponent coupling is $V_{12} = V_{13} = V_{23} = -0.6$.

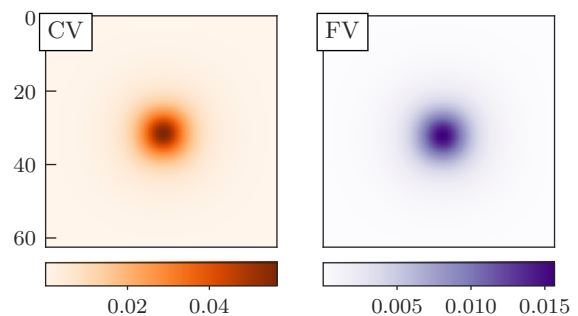


FIG. 6. Magnetic field for conventional (CV) and fractional (FV) vortices in $U(1)^3$ system. Simulation parameters are the same as on FIG. 5. Both vortices have rotational symmetry.

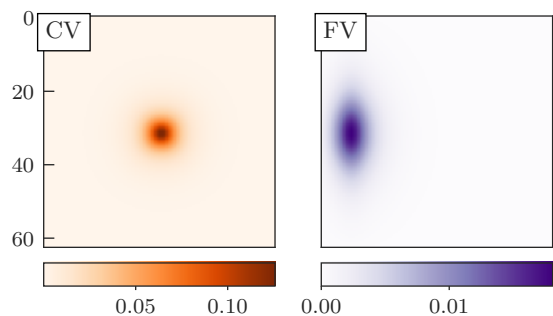


FIG. 7. Magnetic field for conventional (CV) and fractional (FV) vortices in $U(1) \times Z_2$ system. Note that despite the difference in the field amplitude, the localization of the magnetic field of the fractional vortex is different. The model parameters are the same as on FIG. 5. The fractional vortex is elongated along the domain wall.

the existence of these objects by standard symmetry- and topology-based arguments; hence, microscopic justification is especially important. This paper studied the solutions for fractional vortices and domain walls in a fully microscopic three-band Bogoliubov-de-Gennes model, including a fully self-consistent solution for magnetic fields. We find stable vortices whose magnetic field shape, localization, and density-of-states signatures significantly differ from the single-quanta vortices and can be directly probed in experiments. In the model of $s + is$ superconductors, we find that domain walls give a signature in density-of-states. However, this signature is parameters-dependent and may be undetectable. The experimental characterization of these vortices is important also because enclosing a variable fraction of the flux quantum

makes them realize the charge-flux-tube bound state [11]. Hence, these objects obey fractional statistics. Another application for these objects is fluxonics [34, 35].

ACKNOWLEDGMENTS

We thank A. Benfenati and M. Barkman for insightful discussions and providing the code developed in [9]. This work was supported by the Swedish Research Council Grants 2022-04763, by Olle Engkvists Stiftelse, and the Wallenberg Initiative Materials Science for Sustainability (WISE) funded by the Knut and Alice Wallenberg Foundation.

-
- [1] F. London, On the problem of the molecular theory of superconductivity, *Phys. Rev.* **74**, 562 (1948).
- [2] F. London, *Superfluids: Macroscopic theory of superconductivity*, Vol. 1 (Dover Publications, 1950).
- [3] V. L. Ginzburg and L. D. Landau, On the Theory of superconductivity, *Zh. Eksp. Teor. Fiz.* **20**, 1064 (1950).
- [4] L. Gorkov, Microscopic derivation of the ginzburg-landau equations in the theory of superconductivity, *Sov. Phys. JETP* **36**, 1364 (1959).
- [5] Note that no such penalty exists in mesoscopic samples. Also, layered systems and systems with phase jumps at grain boundaries and weak links have geometric effects that can affect enclosed flux; here, we do not discuss such geometric effects.
- [6] M. Sigrist and K. Ueda, Phenomenological theory of unconventional superconductivity, *Rev. Mod. Phys.* **63**, 239 (1991).
- [7] G. E. Volovik, Monopoles and fractional vortices in chiral superconductors, *Proceedings of the National Academy of Sciences* **97**, 2431 (2000).
- [8] E. Babaev, Vortices with fractional flux in two-gap superconductors and in extended faddeev model, *Phys. Rev. Lett.* **89**, 067001 (2002).
- [9] Y. Iguchi, R. A. Shi, K. Kihou, C.-H. Lee, M. Barkman, A. L. Benfenati, V. Grinenko, E. Babaev, and K. A. Moler, Superconducting vortices carrying a temperature-dependent fraction of the flux quantum, *Science* **380**, 1244 (2023).
- [10] Y. Zheng, Q. Hu, H. Ji, I. Timoshuk, H. Xu, Z. Wang, Y. Li, Y. Gao, X. Yu, R. Wu, X. Lu, K. Kihou, V. Grinenko, E. Babaev, N. F. Q. Yuan, B. Lv, C.-M. Yim, and H. Ding, [Direct observation of quantum vortex fractionalization in multiband superconductors](#) (2024), [arXiv:2407.18610](#).
- [11] F. Wilczek, Quantum mechanics of fractional-spin particles, *Phys. Rev. Lett.* **49**, 957 (1982).
- [12] C. Nayak, S. H. Simon, A. Stern, M. Freedman, and S. Das Sarma, Non-abelian anyons and topological quantum computation, *Rev. Mod. Phys.* **80**, 1083 (2008).
- [13] A. Shapere and F. Wilczek, *Geometric phases in physics*, Vol. 5 (World scientific, 1989).
- [14] J. Leinaas and J. Myrheim, On the theory of identical particles, *Il nuovo cimento* **37**, 132 (1977).
- [15] V. Grinenko, P. Materne, R. Sarkar, H. Luetkens, K. Kihou, C. H. Lee, S. Akhmadaliev, D. V. Efremov, S.-L. Drechsler, and H.-H. Klauss, Superconductivity with broken time-reversal symmetry in ion-irradiated $\text{Ba}_{0.27}\text{K}_{0.73}\text{Fe}_2\text{As}_2$ single crystals, *Phys. Rev. B* **95**, 214511 (2017).
- [16] V. Grinenko, R. Sarkar, K. Kihou, C. Lee, I. Morozov, S. Aswartham, B. Büchner, P. Chekhonin, W. Skrotzki, K. Nenkov, *et al.*, Superconductivity with broken time-reversal symmetry inside a superconducting s-wave state, *Nature Physics* **16**, 789 (2020).
- [17] V. Grinenko, D. Weston, F. Caglieris, C. Wuttke, C. Hess, T. Gottschall, I. Maccari, D. Gorbunov, S. Zherlitsyn, J. Wosnitza, *et al.*, State with spontaneously broken time-reversal symmetry above the superconducting phase transition, *Nature Physics* **17**, 1254 (2021).
- [18] I. Shipulin, N. Stegani, I. Maccari, K. Kihou, C.-H. Lee, Y. Li, R. Hühne, H.-H. Klauss, M. Putti, F. Caglieris, *et al.*, Calorimetric evidence for two phase transitions in $\text{Ba}_1\text{-xkfe}_2\text{as}$ with fermion pairing and quadrupling states, *Nature Communications* **14**, 6734 (2023).
- [19] T. A. Bojesen, E. Babaev, and A. Sudbø, Time reversal symmetry breakdown in normal and superconducting states in frustrated three-band systems, *Phys. Rev. B* **88**, 220511 (2013).
- [20] T. A. Bojesen, E. Babaev, and A. Sudbø, Phase transitions and anomalous normal state in superconductors with broken time-reversal symmetry, *Phys. Rev. B* **89**, 104509 (2014).
- [21] I. Maccari and E. Babaev, Effects of intercomponent couplings on the appearance of time-reversal symmetry breaking fermion-quadrupling states in two-component london models, *Phys. Rev. B* **105**, 214520 (2022).
- [22] J. Garaud and E. Babaev, Domain walls and their experimental signatures in $s + is$ superconductors, *Phys. Rev. Lett.* **112**, 017003 (2014).
- [23] A. Benfenati, M. Barkman, and E. Babaev, Demonstration of $\mathbb{C}P^2$ skyrmions in three-band superconductors by self-consistent solutions of a bogoliubov-de gennes model, *Phys. Rev. B* **107**, 094503 (2023).
- [24] R. Peierls, Zur theorie des diamagnetismus von leitungs-elektronen, *Zeitschrift für Physik* **80**, 763 (1933).

- [25] R. P. Feynman, R. B. Leighton, and M. Sands, *The Feynman lectures on physics, Vol. I: The new millennium edition: mainly mechanics, radiation, and heat*, Vol. 1 (Basic books, 2011).
- [26] V. Stanev and Z. Tesanovic, Three-band superconductivity and the order parameter that breaks time-reversal symmetry, *Phys. Rev. B* **81**, 134522 (2010).
- [27] J. Böker, P. A. Volkov, K. B. Efetov, and I. Eremin, $s + is$ superconductivity with incipient bands: Doping dependence and stm signatures, *Phys. Rev. B* **96**, 014517 (2017).
- [28] F. Gygi and M. Schluter, Electronic tunneling into an isolated vortex in a clean type-ii superconductor, *Phys. Rev. B* **41**, 822 (1990).
- [29] F. Gygi and M. Schluter, Angular band structure of a vortex line in a type-ii superconductor, *Phys. Rev. Lett.* **65**, 1820 (1990).
- [30] F. Gygi and M. Schlüter, Self-consistent electronic structure of a vortex line in a type-ii superconductor, *Phys. Rev. B* **43**, 7609 (1991).
- [31] H. F. Hess, R. B. Robinson, and J. V. Waszczak, Vortex-core structure observed with a scanning tunneling microscope, *Phys. Rev. Lett.* **64**, 2711 (1990).
- [32] O. Fischer, M. Kugler, I. Maggio-Aprile, C. Berthod, and C. Renner, Scanning tunneling spectroscopy of high-temperature superconductors, *Rev. Mod. Phys.* **79**, 353 (2007).
- [33] E. Babaev, J. Jäykkä, and M. Speight, Magnetic field delocalization and flux inversion in fractional vortices in two-component superconductors, *Phys. Rev. Lett.* **103**, 237002 (2009).
- [34] K. Miyahara, M. Mukaida, and K. Hohkawa, Abrikosov vortex memory, *Applied Physics Letters* **47**, 754 (1985).
- [35] T. Golod, A. Iovan, and V. M. Krasnov, Single abrikosov vortices as quantized information bits, *Nature Communications* **6**, 8628 (2015).